J Mater Sci (2020) 55:11367–11381

Computation & theory

Electronic and mechanical properties of silicene after nuclear transmutation doping with phosphorus

Alexander Y. Galashev[1,2,*] and Alexey S. Vorob'ev[1]

[1] Institute of High-Temperature Electrochemistry, Ural Branch, Russian Academy of Sciences, Sofia Kovalevskaya Str. 22, Yekaterinburg, Russia 620990

[2] Ural Federal University named after the first President of Russia B.N. Yeltsin, Mira Str., 19, Yekaterinburg, Russia 620002

Received: 14 February 2020
Accepted: 20 May 2020
Published online: 3 June 2020

ABSTRACT

The present work is aimed at studying the changes in the electronic and mechanical properties of silicene as a result of its doping with phosphorus. It is proposed to use modified silicene as the material of the anode of a lithium-ion battery. The performed first-principle calculations of the density spectrum of electronic states show that silicene on a graphite substrate after neutron transmutation doping is converted from a narrow-gap semiconductor into a material having metallic conductivity. The influence of the composition of the alloyed material on adhesion energy and the possible types of binding energy is investigated. The molecular dynamics method was used to study the intercalation of lithium in doped silicene channel located on a modified graphite substrate. The straightening of corrugated silicene using alloying can significantly increase the capacity for filling the modified channel with lithium. Despite a more than twofold increase in channel volume during lithization, it retains strength and high capacity if the phosphorus content in silicene does not exceed 6%. In this case, the stresses arising in the walls of the channel from doped silicene are not critical.

Introduction

Recently, the study of the properties of two-dimensional materials has become increasingly relevant. For functionalized graphene and graphene-based composite materials, a variety of applications are proposed. They are proposed to be used for hydrogen storage [1], as sensors/actuators and soft robots [2], composite catalysts [3], etc. Often, the decisive factors for the use of these materials are good heat and electricity conductivity of graphene, as well as its large modulus of elasticity. However, in the presence of defects, which, for example, inevitably appear upon receipt of graphene by reduction of its oxide, graphene in many ways loses its remarkable properties. In [4], a physical method is proposed for eliminating vacancy defects in graphene. In the band structure of freestanding silicene, the Dirac cone characteristic of graphene is reproduced. The range

Address correspondence to E-mail: galashev@ihte.uran.ru

https://doi.org/10.1007/s10853-020-04860-8

of useful electronic properties of silicene is even wider than that of graphene. A fairly easy adjustment of the band gap in silicene is its most important advantage over graphene. This suggests its widespread use in nanoelectronics.

Doping with impurities is used to significantly change the electrical and optical properties of silicon material. As a result of doping in the band gap of the semiconductor, impurity states are created that affect its physical properties. By adjusting the doping levels, the necessary values of the electrical and photoluminescent properties can be achieved [5, 6]. The nuclear spin of a ^{31}P impurity of an atom replacing a silicon atom is used as a quantum bit [7, 8]. Therefore, the enhancement of the hyperfine splitting of P-impurities contained in a silicon material [9] is extremely important for the implementation of quantum information processing. Impurity effect plays an important role on the conductivity of a thin silicon crystalline film [10].

Recently, many works have been performed aimed at studying the possibility of using silicene as the anode material of lithium-ion batteries [11–17]. Silicon is considered as the most suitable anode material for LIB because the battery capacity when using it can be increased from 372 mA h g^{-1}, typical for a graphite anode, to 4200 mA h g^{-1}. This is due to the ability of the Si atom to retain during intercalation up to 4.4 Li atoms. Another important requirement for the anode material is its strength and ability to withstand a large number of battery charge/discharge cycles. Bulk crystalline silicon is not suitable material for the LIB anode. Despite its ability to contain a large number of lithium atoms during intercalation, it does not withstand prolonged cycling.

The elastic stiffness of the silicene monolayer is 50.44 N m^{-1} for the zigzag direction and 62.31 N m^{-1} for the chair direction. The tensile strength of silicene (5.85 N m^{-1}) is $\sim$ 3 times higher, and the critical tensile strain (18%) is more than an order of magnitude higher than that of crystalline silicon [18]. In its strength properties, silicene is inferior to graphene and exhibits fracture characteristics different from graphene. In particular, if graphene is torn only along its zigzag edge, then silicene can be split both along the zigzag edge and along the edge of the armchair [19].

It was shown in [20–23] that it is advantageous to use silicene filled with vacancy defects as an anode. In this case, the capacitance of the electrode increases significantly. Moreover, for reasons of mechanical strength, it is necessary to limit oneself to silicene having mono- or bivacancies [12–14]. The charge capacity decreases if the silicene anode has defects such as tri- and hexavacancies. The presence of a strong corrugation prevents the effective use of silicene as anode material. Due to the high height of the silicene buckles (when silicene located on the metal surface), the entry of lithium ions into the gap formed by the silicene sheets is difficult.

The experimentally obtained silicene on a metal (Ag, Ir, Au) [24–26] or nonmetallic (MoS_2, glassy carbon, or graphite) [27–29] substrate cannot be separated from this substrate. This is explained by the high exfoliation energy, the calculation method by which using semi-infinite substrates were proposed in [30]. Therefore, the use of silicene in LIB is possible only together with the substrate on which it is obtained. Moreover, in [26], graphene-like silicene sheets were synthesized for the first time, i.e. flat silicene. Silicene on a graphite substrate can be considered as a contender for use in the design of the anode LIB, which has a high charge capacity. Silicene is a narrow-gap semiconductor having a band gap of $\sim$ 27 meV [26]. However, silicene on the substrate can acquire metallic conductivity. Increasing the electrical conductivity of the anode material will increase the speed of charging and discharging the LIB and make the battery more attractive to use. Local changes in the structure of silicene can protect against changes in electronic properties caused by the influence of a metal substrate [31].

Doping of silicene with phosphorus (by an element of group V) introduces additional uncompensated electrons into the system and, under heavy doping, should significantly increase its electrical conductivity. In addition, it was experimentally established that, in silicon doped with phosphorus, the Si–P bond strength is higher than that of the Si–Si bond [32]. In [33], it was shown that the strength of graphene (graphite sheet) increases when it is doped with nitrogen. Using nuclear transmutation doping (NTD), you can replace part of Si atoms to P atoms and part C atoms to N atoms in one thermal neutron irradiation session. Therefore, there is reason to believe that using the NTD method, it is possible to increase the electrical conductivity of silicene without decreasing its strength.

The purpose of this work is to study the electronic and mechanical properties of the system "silicene on a graphite substrate" subjected to nuclear transmutation doping in order to establish the possibility of its use both in nanoelectronics and as an anode material of LIB.

Materials and methods

The electronic properties of modified silicene were calculated using the Siesta [34] software package. In this paper, we consider the effect of neutron irradiation of silicene on a carbon substrate. During such irradiation in silicene, some silicon atoms are transformed into phosphorus atoms. Silicene presented in two ways: a single-layer is a 2 × 2 supercell (eight silicon atoms located in two *xy* planes) and a two-layer—two 2 × 2 silicene supercells (sixteen silicon atoms in four *xy* planes). The thickness of the carbon substrate was selected using additional computer simulation. Substrates consisting of one to four graphite layers were considered. One substrate layer was defined by 18 carbon atoms, i.e., supercell 3 × 3. The "silicene–carbon substrate" system were geometrically optimized. The initial distance between the layers of the graphite substrate was 0.3314 nm. The calculations used periodic Born–Karman boundary conditions implemented in the Siesta program. The translation parameters for the graphene and silicene supercells used were 0.741 nm and 0.774 nm, respectively. The translation parameter in the *x* and *y* directions for the combined silicene–graphite supercell was chosen equal to 0.7575, i.e. corresponded to a similar value used in [35], which shows the preservation of electronic properties of both freestanding silicene and graphene in a combined supercell. Thus, the system used was an infinitely translated short-period superlattice. The translation vector in the *z* direction was chosen equal to 35 Å.

Doping was carried out by replacing silicon atoms with phosphorus atoms and carbon atoms with nitrogen atoms. When studying a mono- and bilayer of silicene on a graphite substrate, from 1 to 2 silicon atoms were replaced. Such substitution was performed at all possible atomic locations in silicene, including its upper and lower sublattices. Substitution from 1 to 2 C atoms was carried out only in the upper sheet of the substrate. The replacement was carried out randomly, without the possibility of forming an N–N bond. All calculated characteristics were averaged over the sets of the systems under consideration. Band structures and electronic state spectra (DOS) were determined. For our system with layered geometry, the van der Waals interactions can have a significant impact on the determination of the energy characteristics [36, 37]. Therefore, systems have been geometrically optimized using van der Waals density function (VdW-DF) DRSLL approximation approach considered in [38] by Dion et al. Dynamic relaxation of atoms was carried out until the change in the total energy of the system became less than 0.01 meV. The atom's structure was relaxed until the remaining forces were less than 20 meV/Å. The cutoff energy of the plane wave basis was assumed to be 200 Ry. The Brillouin zone was set by the Monhorst–Pack method using 10 × 10 × 1 k-points.

The adhesion energy between the graphite substrate and silicene was calculated according to

$$E_{\mathrm{ad}} = \frac{-\left(E_{\mathrm{tot}} - E_{\mathrm{Si(P)}} - E_{\mathrm{C(N)}}\right)}{n_{\mathrm{cell}}}, \tag{1}$$

where E_{tot} is the total energy of the entire system, $E_{\mathrm{Si(P)}}$ is the total energy of silicene (not irradiated or doped with phosphorus), $E_{\mathrm{C(N)}}$ is the total energy of the carbon substrate (not irradiated or doped with nitrogen), and n_{cell} is the number of unit cells in the silicene supercell. In this case, the phosphorus and nitrogen atoms in the system were considered as belonging to the silicene supercell and carbon substrate, respectively.

We calculated two binding energies: (1) in silicene and (2) in a graphite substrate. The expression for calculating the binding energies:

$$E^{\mathrm{b}}_{(\mathrm{Si(P)/C(N)})} = \frac{-(E_{\mathrm{tot}} - n_{\mathrm{Si/C}}E_{\mathrm{1Si/1C}} - n_{\mathrm{P/N}}E_{\mathrm{1P/1N}} - E_{\mathrm{C(N)/Si(P)}})}{n_{\mathrm{Si(P)/C(N)}}}, \tag{2}$$

where $E_{\mathrm{1Si/1C}}$ and $E_{\mathrm{1P/1N}}$ are the total energies calculated for one silicon or carbon atom and phosphorus or nitrogen atom, respectively; $n_{\mathrm{Si/C}}$ and $n_{\mathrm{P/N}}$ are the number of Si or C and P or N atoms in the system, $n_{\mathrm{Si(P)/C(N)}}$ is the number of atoms in modified silicene or carbon substrate.

Our method for calculating the stress distribution in silicene sheets is as follows. We divide the sheets of silicene into elementary areas with the normal γ (x, y, z) and elongated either in the "armchair" direction or in the "zigzag" direction. Next, the resulting force

acting on each of the areas is determined. In determining the resultant force, only those interactions between particles i and j are taken into account, the force vector of which pierces the given area [39]. In addition, the calculation of $\sigma_{\gamma\alpha}(l)$ takes into account the directions α (x, y, z) of the velocities of the atoms i and j:

$$\sigma_{\gamma\alpha}(l) = \left\langle \sum_{i}^{n} \frac{1}{\Omega} \left(m v_{\gamma}^{i} v_{\alpha}^{i} \right) \right\rangle + \frac{1}{S_l} \left\langle \sum_{i}^{n} \sum_{j \neq i}^{(u_i \leq u, u_j \geq u)} \left(f_{ij}^{\alpha} \right) \right\rangle. \quad (3)$$

In expression (3), the following notation is used: n is the number of atoms on the lth area, Ω is the volume per atom, m is the atomic mass, v_{α}^{i} is the α projection of the velocity of the ith atom, S_i is the area of the lth surface element, f_{ij}^{α} is the α projection of the resulting force from the interaction of i and j atoms that passes though the lth area, and u_i is the coordinate of the atom i; the coordinate of the contact point of the straight line passing through the centers of the atoms i and j and the lth surface element is denoted through the symbol u.

Results

Calculation of electronic properties of the doped "silicene–graphite substrate" system

We performed the calculations of the physical properties of both an autonomous (without a substrate) single- and two-layer silicene (Si), and silicene on a graphite substrate (Si–C). To determine the optimal number of substrate layers, four systems were used containing from 1 to 4 graphene layers in which from 18 to 72 carbon atoms were contained. After geometric optimization of these systems, the adhesion energies characterizing the adhesion between silicene and a carbon substrate were calculated. Table 1 shows the values of adhesion energy depending on the number of layers in a graphite substrate. It is seen that an increase in the thickness of the substrate from two layers to three changes the adhesion energy between the substrate and silicene by about 3% in comparison with the case of single-layer and double-layer silicene. Accounting for four layers of the substrate leads to a difference in E_{ad} from the variant with two layers by no more than 2% in both cases. Therefore, in further calculations, we used a graphite substrate represented by two layers containing 36 carbon atoms.

Figure 1 shows Si–C systems after geometric optimization. During the optimization, noticeable geometric rearrangements occurred in the freestanding, unmodified silicene. As a result, the average distance between the Si-Si_{int} silicene sublattices increased from 0.44 to 0.56 Å and from 0.44 to 1.01 Å for single-layer and double-layer silicene, respectively.

Table 2 presents the energy characteristics of the system. Replacing Si atoms with P atoms leads to an increase from 2 to 4% of the binding energy $\left(E_{Si(P)}^{b}\right)$ in the modified silicene sheet. This indicates an increase in the stability of phosphorus-doped silicene compared to undoped one. While replacing C atoms with N leads to decrease in the binding energy $\left(E_{C(N)}^{b}\right)$ in the modified graphite substrate approximately on 2%. The dependence of the adsorption energy on the number of N and P atoms in the modified system "silicene–carbon substrate" was not detected.

The interplanar distance R_{Si-C} between the carbon substrate and the lower silicene sheet (Si–C) in all cases considered was 3.44 Å. Also, the average Si–C, C–C, Si–P, and C–N bond lengths of 3.64, 1.44, 2.34, and 1.47 Å, respectively, turned out to be independent of the number of phosphorus atoms. The distance between silicon atoms (L_{Si-Si}) in the phosphorus-modified autonomous silicene sheet and in the corresponding silicene layer on the carbon substrate is close to 2.31 Å. In this case, the replacement of silicon atoms by phosphorus atoms in the "monolayer silicene–carbon substrate" system leads

Table 1 The adhesion energy between silicene and a graphite substrate, in the presence of 1–2 sheets in silicene, and from 1 to 4 layers in the substrate, eV un $cell^{-1}$

The quantity of sheets of silicene	The quantity of graphite substrate layers			
	1	2	3	4
1	0.284	0.300	0.309	0.306
2	0.300	0.321	0.328	0.324

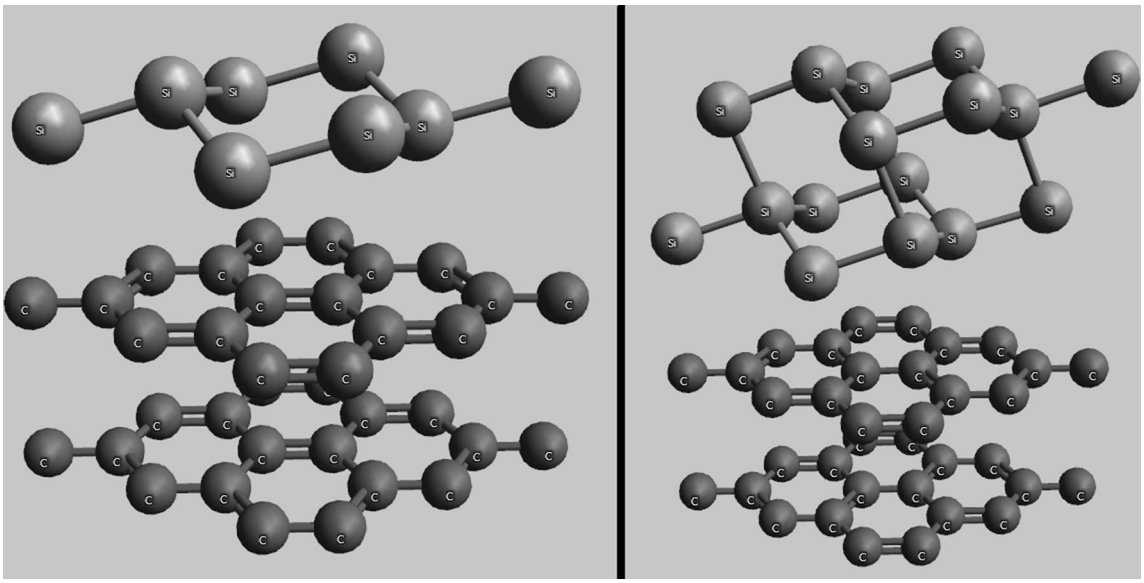

Figure 1 Unmodified silicene on a graphite substrate after geometric optimization.

Table 2 Binding and adsorption energy and the distance between the sublattices of silicene containing from 0 to 2 phosphorus atoms on a graphite substrate having from 0 to 2 nitrogen atoms

N_{Si}	N_N	N_P	$E^b_{Si(P)}$ (eV)	$E^b_{C(N)}$ (eV)	E_{ad} (eV un cell^{-1})	R_{Si-Si} (Å)
1	0	0	4.408	8.546	0.300	0.626
		1	4.470	8.549	0.330	0.711
		2	4.513	8.548	0.316	0.790
	1	0	4.416	8.464	0.316	0.630
		1	4.465	8.465	0.318	0.715
		2	4.512	8.464	0.314	0.791
	2	0	4.418	8.379	0.321	0.627
		1	4.511	8.379	0.323	0.716
		2	4.602	8.464	0.318	0.789
2	0	0	4.453	8.547	0.321	1.071
		1	4.539	8.546	0.303	1.084
		2	4.547	8.512	0.296	1.053
	1	0	4.451	8.446	0.325	1.042
		1	4.457	8.464	0.316	0.997
		2	4.501	8.464	0.316	1.038
	2	0	4.444	8.378	0.327	0.951
		1	4.445	8.375	0.322	1.045
		2	4.478	8.377	0.301	1.074

to an increase in the distance between the silicene sublattices from 0.626 to 0.791 Å. In bilayer silicene, the L_{Si-Si} bond length increases to 2.38 Å. The increase in the L_{Si-Si} bond lengths is caused by an increase in the R_{Si-Si} distance between the silicene sublattices to about 1 Å. The dependence of the L_{Si-Si} bond length and the distance between the R_{Si-Si} silicene sublattices on the number of nitrogen atoms in the carbon substrate was not found.

The calculated projected densities of states (Fig. 2) predict that freestanding, pristine silicene is a semiconductor with a band gap of 35 meV, while silicene on a graphite substrate is a conductor. Our calculations show that autonomous bilayer silicene is a semiconductor with band gap equal to 131 meV. The reason of electronic conductivity in single- and bilayer silicene on the graphite substrate is interaction between silicon and carbon atoms. As can be seen from Fig. 2, the conductivity arises due to the

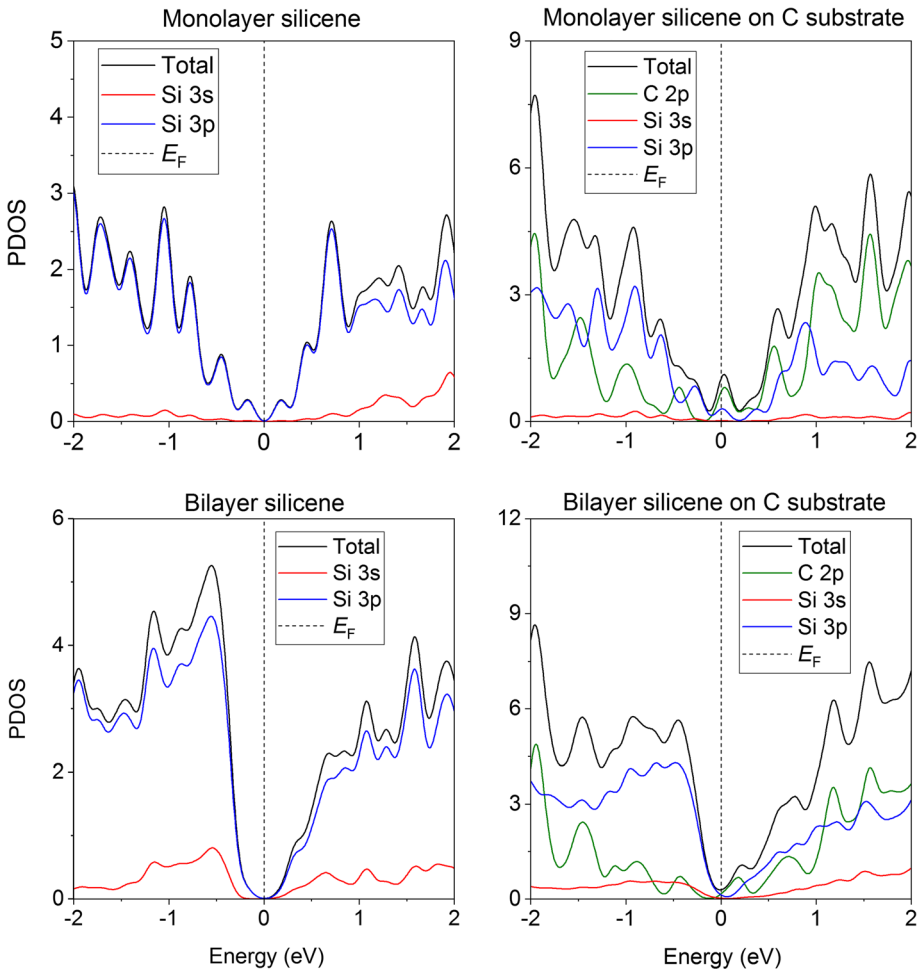

Figure 2 Projected densities of states of a single-layer and two-layer silicene: on the left—autonomous silicene, on the right—silicene on a graphite substrate.

interaction of 2p carbon electrons with 3p electrons of silicene, which is consistent with the data of [40, 41].

Figure 3 shows examples of projected densities of states of the system "monolayer silicene–carbon substrate" depending on the modification of this system by phosphorus and nitrogen atoms. All obtained systems retain conductor properties regardless of the number and arrangement of phosphorus atoms in the silicene sheet and nitrogen atoms in the carbon substrate.

Figure 4 shows examples of projected densities of states of the "bilayer silicene–carbon substrate" system, depending on the modification of this system by phosphorus and nitrogen atoms. All systems containing nitrogen in a carbon substrate or containing one phosphorus atom in silicene sheets are conductors. However, we found configurations of the "bilayer silicene–carbon substrate" system containing two phosphorus atoms with semiconductor properties.

Figure 5 shows the projected densities of states of the "bilayer silicene–carbon substrate" system when replacing from 0 to 2 carbon atoms with nitrogen ones, as well as replacing two silicon atoms with phosphorus ones. It can be seen that when 1 to 2 carbon atoms in the graphite substrate are replaced by nitrogen atoms, the Fermi level shifts and the conductivity along the p level of carbon increases. In the absence of nitrogen atoms in the carbon substrate, semiconductivity with a band gap of 0.009–0.023 eV is possible. The occurrence of semiconductivity is associated with the position of phosphorus atoms in silicene. Thus, the "bilayer silicene–carbon substrate" system acquires semiconductor properties when two silicon atoms are replaced in the following positions: 1. Two atoms in the lower sublattice of the bottom silicene sheet; 2. One atom in the lower sublattice of the bottom layer and one atom in the lower sublattice of the upper silicene sheet; 3. One atom in the lower and one atom upper sublattice of the bottom sheet of

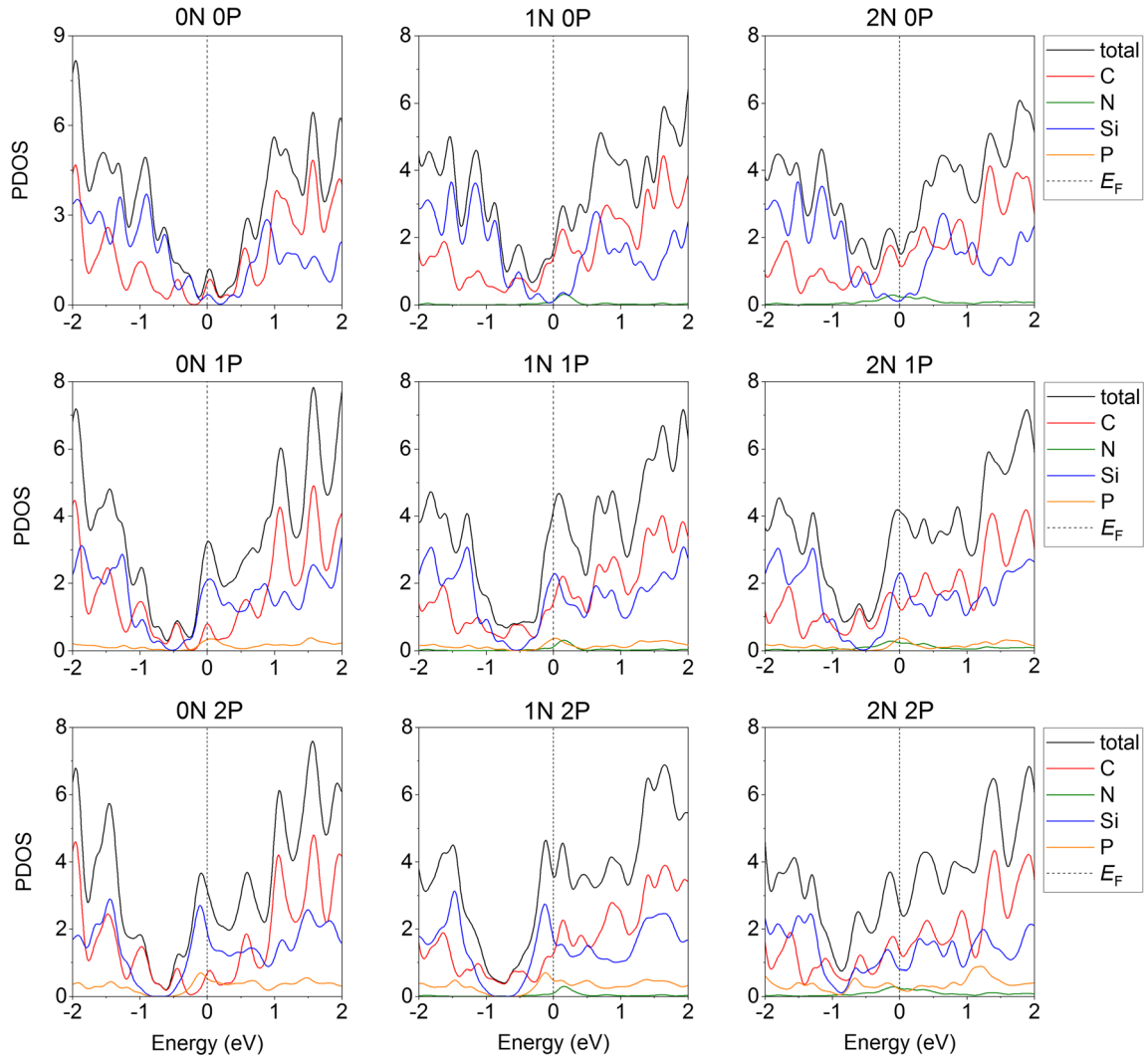

Figure 3 Projected densities of states of modified systems of "monolayer silicene on a graphite substrate" in which a silicene sheet contains from 0 to 2 P atoms, and a graphite substrate contains from 0 to 2 N atoms.

silicene; 4. One atom in the lower sublattice of the bottom layer and one atom in the upper sublattice of the upper silicene sheet. Wherein, all configurations have a similar form of PDOS, however, differing on the value of the band gap.

Stresses in modified silicon channel filled with lithium

Using the classical molecular dynamics method considered in Supplementary information, lithium filling of silicene channels on a graphite substrate was studied before and after using the NTD method to modify this two-dimensional material. The configurations of two of the systems considered here after the channel is filled to the maximum with lithium are shown in Fig. 6. The modified silicene in Fig. 6 (right) had 3% doping with phosphorus, and its graphite substrate had 5% doping with nitrogen.

Figure 7 shows the xy-projections of the upper sheets of silicene obtained by the maximum filling of the channel with lithium in the case of 3% and 9% doping of silicene with phosphorus. Li atoms occupy the upper half of the channel, i.e., cutoff by a horizontal plane drawn through the middle of the height of the channel. At 3% doping, P atoms are always separated from each other, located below the main plane of the silicene sheet and, as a rule, are bound to 3 Si atoms. In the case of 9% doping, P atoms are also located under a silicene sheet, can be located separately from each other or have a P–P bond. Phosphorus atoms are bound to both three and four Si

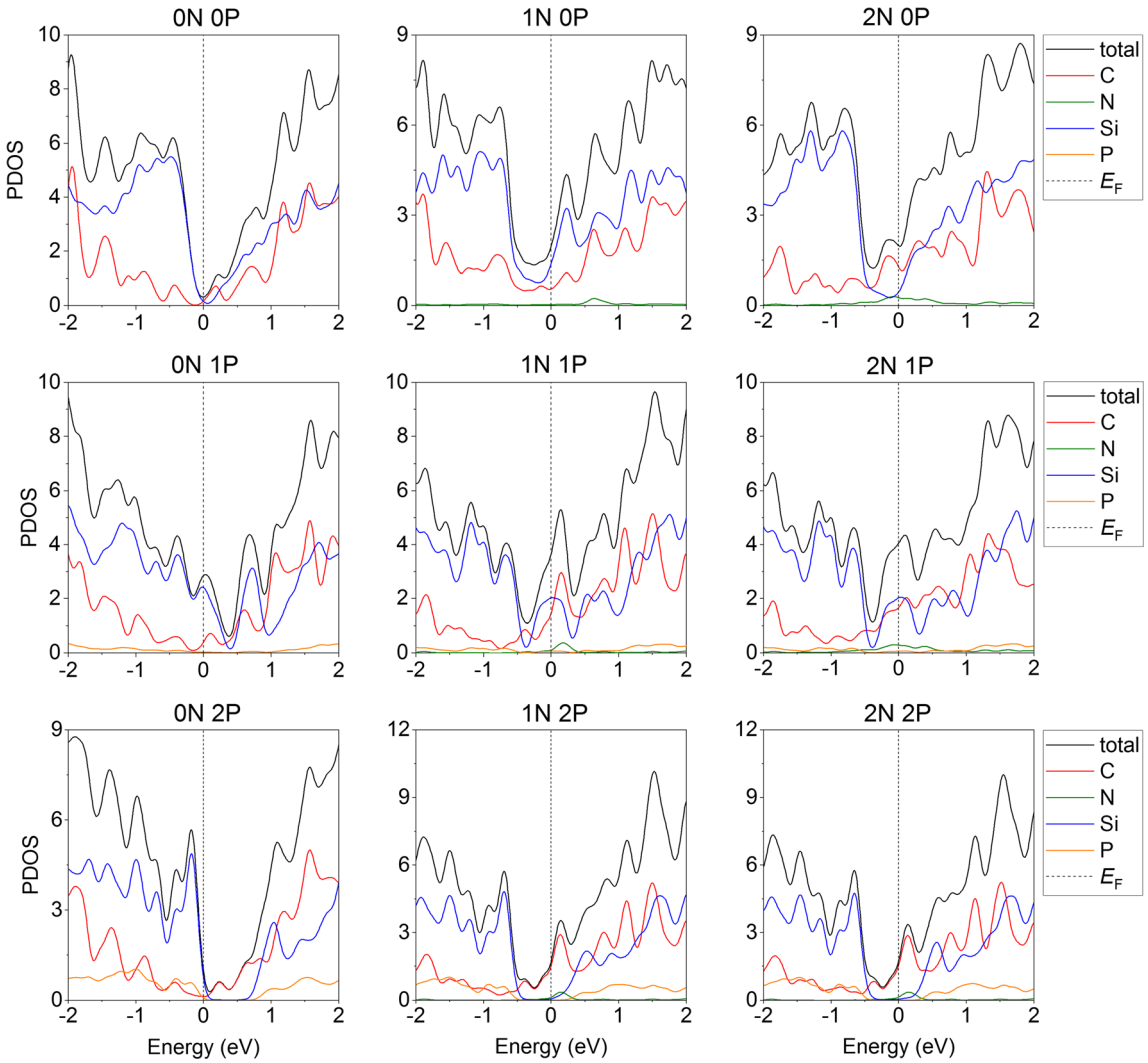

Figure 4 Projected densities of states of modified systems of "bilayer silicene on a graphite substrate" in which a silicene sheet contains from 0 to 2 P atoms, and a graphite substrate contains from 0 to 2 N atoms.

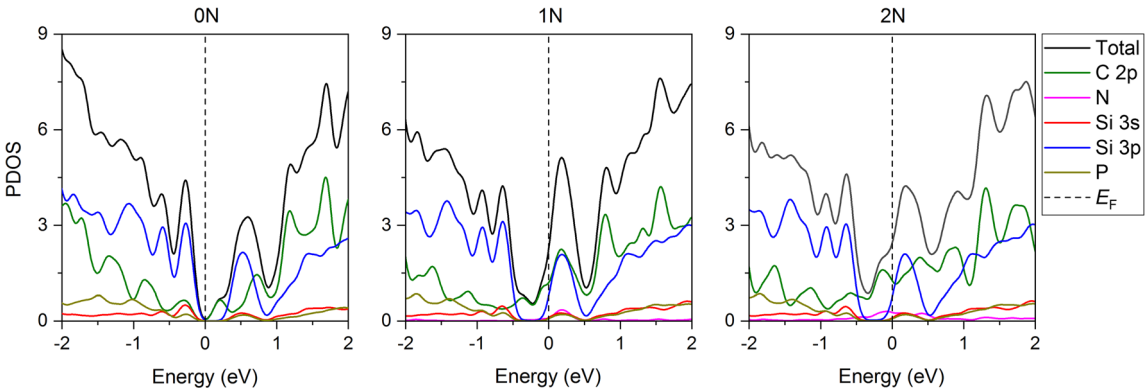

Figure 5 Projected densities of states of modified systems of "bilayer silicene on a graphite substrate" in which a silicene sheet contains 2 P atoms, and a graphite substrate contains from 0 to 2 N atoms.

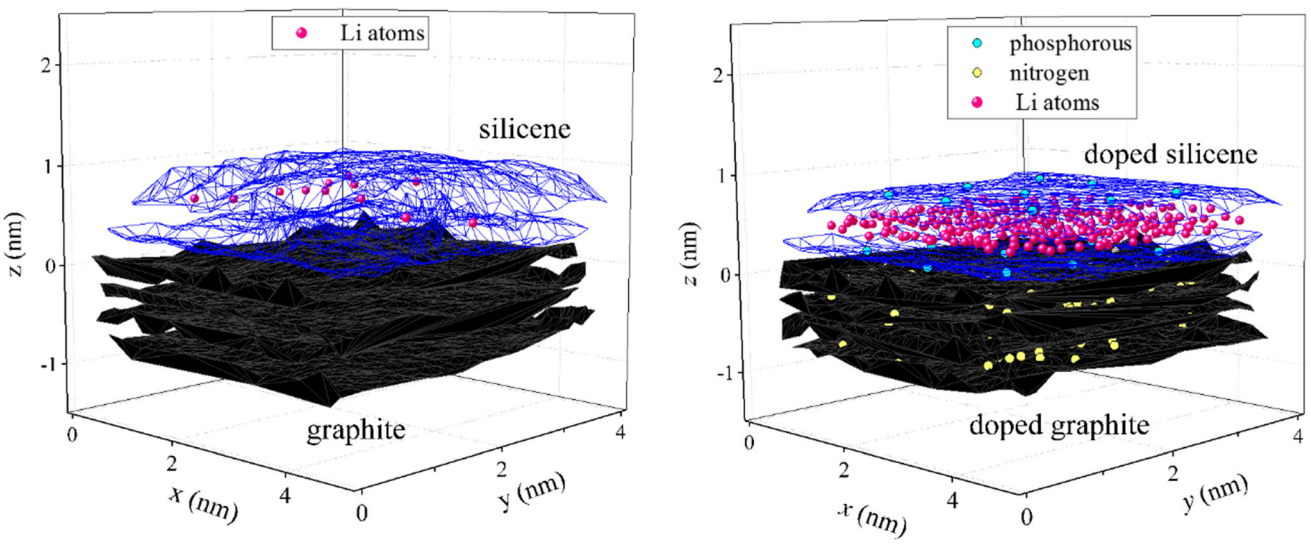

Figure 6 A lithium-filled silicene channel with a gap between sheets of 0.24 nm after 500 ps for an undoped (left) and doped system (right).

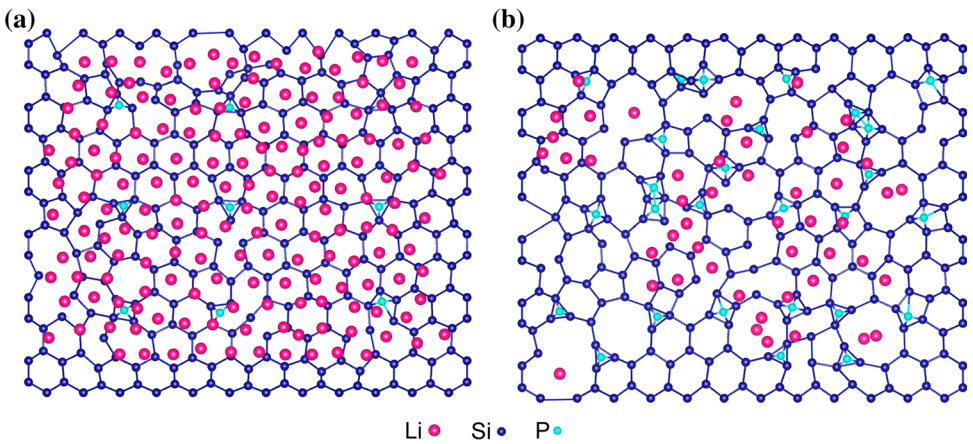

Figure 7 Xy projections of the upper sheets of silicene doped with phosphorus, with lithium atoms belonging to these sheets: **a** 3% doping, **b** 9% doping; Li atoms falling into the upper part of the silicene channel at the maximum filling of the channel with lithium are shown.

atoms. At 3% doping, large pores are practically absent in silicene and the channel has a high filling with lithium, while at 9% doping there are a lot of such pores, and the channel filling is low. In addition, at 9% and 18% doping, weak (strongly stretched) Si–Si bonds are present in silicene sheets.

The limiting number of lithium atoms intercalated into a silicene channel depending on the channel width for 3% P-doped and undoped silicene is presented in Table 3. It can be seen that the introduction of phosphorus into silicene allows a larger number of lithium atoms to be introduced into the channel.

Table 4 shows the values of the maximum number of Li atoms intercalated into a channel with a gap of 0.24 nm for various degrees of doping of silicene. In the absence of doping, Li atoms hardly enter the silicene channel. However, in the presence of monovacancies initially occupied by P atoms, the filling of the channel with lithium increases sharply. It can be seen that the largest number of Li atoms filling the channel is achieved with 6% doping of silicene with phosphorus. The channel filling by

Table 3 The maximum number of lithium atoms obtained as a result of intercalation in undoped ($N_{Li\ (pristine)}$) and 3% P-doped ($N_{Li\ (NTD)}$) silicene channels depending on the gap width h_g between the channel forming sheets

N	h_g (nm)					
	0.24	0.35	0.45	0.55	0.65	0.75
$N_{Li\ (pristine)}$	12	25	13	13	21	143
$N_{Li\ (NTD)}$	244	183	146	149	156	165

Table 4 The maximum number of lithium atoms obtained as a result of intercalation in P-doped ($N_{Li\ (NTD)}$) silicene channels depending on the degree of doping

N	N_P (%)				
	0	3	6	9	18
$N_{Li\ (NTD)}$	12	244	271	72	72

lithium is significantly reduced when P atoms were initially inserted into tri- and hexavacancies in silicene. This is due to the fact that, over time, getting inside the channel, P atoms restrain the filling of the channel with lithium.

The nature of the average elastic stresses appearing in the channel walls reflects the stress tensor $\sigma_{\gamma\alpha}$ calculated according to the formula (3). The stress tensor was calculated throughout the entire intercalation period. The stresses averaged over both silicene sheets from the forces acting in the xy plane and perpendicular to this plane at a channel gap of 0.24 nm are shown in Fig. 8. Stresses σ_{zz} acting in silicene at the entrance to the channel seem to be the most significant. Blocking the channels at the inlet, especially with defects in the form of tri- and hexavacancies, allows you to unload the areas of the channel walls close to its entrance (here, σ_{zy} and σ_{zz} are minimal). The most uniform stress distribution σ_{zz} is achieved when moving along the $0x$ direction ("zigzag"), when the channel walls contain monovacancies initially filled with P atoms. When moving along the $0y$ axis, not only the inhomogeneity of σ_{zz} stresses but also σ_{zy} stresses increases. Due to the very thin bridges between the pores formed in silicene with 18% phosphorus doping, the transition from elastic to inelastic deformation during cycling occurs very quickly (less than 1 ps). In this case, the breaking of Si–Si bonds in the bridging region lead to the destruction of the silicene sheet.

The introduction of lithium into the channel leads to an increase in the volume of space enclosed between the sheets of two-dimensional material that form it, i.e. channel volume. Figure 9 shows the V_i/V_0 volume ratio of the channel formed by sheets of pure perfect silicene (undoped), as well as V_i/V_0 for channels in the walls of which P atoms initially filled mono-, bi-, tri-, and hexavacancies. The volume of the channel filled with lithium is indicated as V_i, and the volume of the original empty channel as V_0. As can be seen from Fig. 9, the largest increase in channel volume occurs at 6% doping of silicene with phosphorus, and the smallest—at 18% doping. In the case of 6% doping, the highest filling of the channel with lithium was observed; at 9% and 18% doping, the filling of the channel was restrained due to the presence of P atoms inside the channel. Bound by a strong bond with Si atoms, P atoms were surrounded by Li atoms entering the channel. As a result, the number of Li atoms intercalated into the channel decreased and the channel volume decreased.

Discussion

In this work, we showed that the graphite substrate promotes the appearance of conductive properties in silicene. The full two-dimensional Si–C system, subjected to the NTD procedure, retains the conductive properties of the silicene film on a graphite substrate. The return of the electronic properties of such a system to the properties of a narrow-gap semiconductor is possible only in exotic cases, when only the silicon part of the Si–C system is doped, and only at a certain concentration of phosphorus in silicene. The appearance of conductive properties in silicene favors its use as an anode material of LIB. It was important to establish how strong stresses appear in silicene sheets during intercalation of lithium atoms into the space created by sheets. If the local stresses in silicene are moderate and allowable for its operation, and the contained amount of lithium is not inferior to the corresponding value obtained when silicene was on metal substrates, then the NTD procedure will bring a positive effect.

Modeling of the channel filling with lithium showed that a silicene channel subjected to 3% doping with phosphorus contains significantly more Li atoms than a similar channel from pristine silicene. This difference is especially noticeable with a small channel gap. So, if the channel with a gap of 0.24 nm, subjected to the NTD procedure, contains 20 times more lithium atoms than the channel of pristine silicene, then with a gap of 0.75 nm the ratio of their capacities is 1.15. A sharp increase in the capacity of the channel irradiated with neutrons is due to smoothing of the channel walls during alloying. Smooth walls not only do not inhibit the influx of Li^+ ions into channel, but also allow the channel to expand easily when it is filled with lithium.

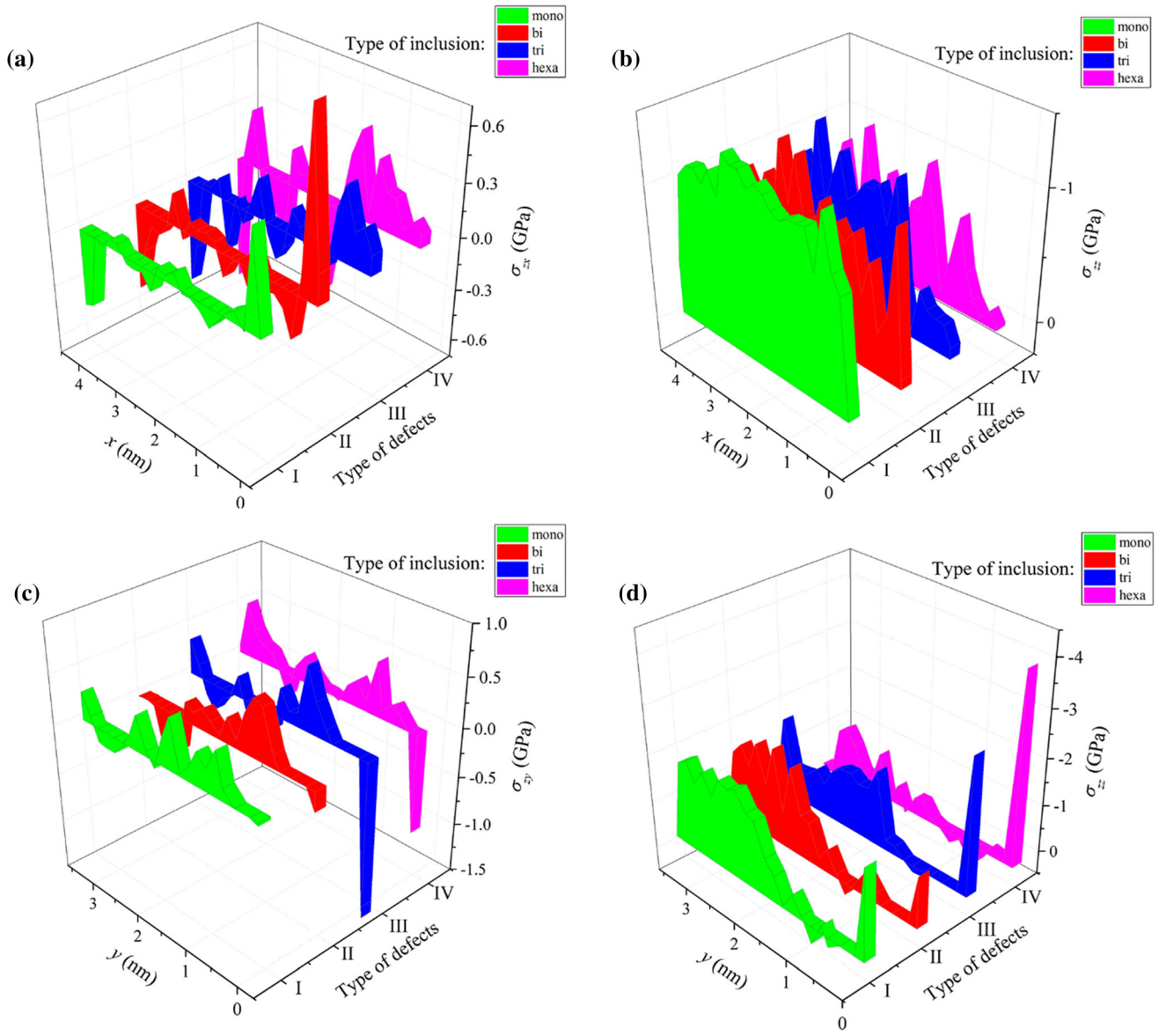

Figure 8 Stress distribution in a lithium-intercalated silicene channel with defects initially filled with P. atoms; the channel with a gap of 0.24 nm is located on a graphite substrate, which has 5% doping with nitrogen; **a**, **b** show the distribution of stresses σ_{zx} and σ_{zz} along the direction 0x (zig–zag); **c**, **d** show the distribution of stresses σ_{zy} and σ_{zz} along the direction 0y (armchair); the intercalation time is 520 ps.

To determine the influence of the van der Waals contribution to the interaction of atoms during geometric optimization, we performed similar calculations using a generalized gradient approximation in the form of PBE [42]. For all systems under study, (VdW-DF) DRSLL and PBE optimization methods give the large difference in the calculation of the adsorption energy between silicene and the substrate. The difference (ΔE_{ad}) in this quantity was most pronounced in the case of the system "undoped bilayer silicene on a 2.7% doped graphite substrate", i.e. according to Table 2 for the system (N_{Si} = 2, N_N = 1, N_P = 0), where the adhesion energy in the absence of VdW interactions is 5.4 times lower than E_{ad} in their presence. It is noteworthy that it was for this system that the minimal difference in the $R_{Si–Si}$ value was achieved, calculated in two different ways (1.16% more in the presence of Van der Waals forces). The weakest difference in the energies E_{ad} was obtained per the system (N_{Si} = 1, N_N = 0, N_P = 0), where the adhesion energy in the absence of VdW forces is 2.3 times lower. For the same system, one of the largest

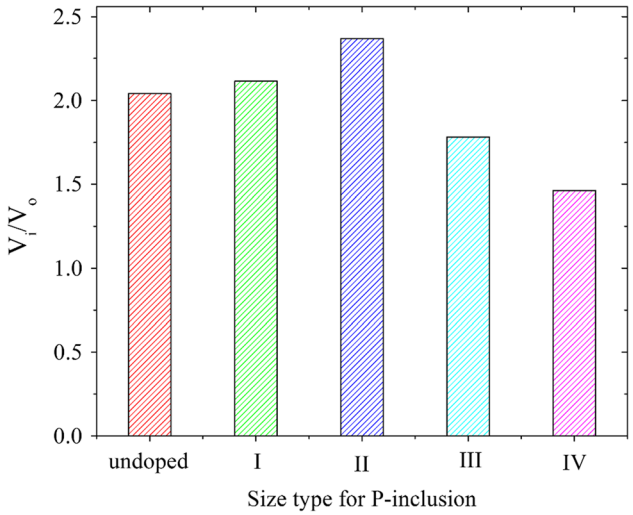

Figure 9 Change in the volume of the modified channel as a result of its filling with lithium. Roman numerals denote the type of vacancy defect filled by P atoms and correspond to the same notation as in Fig. 8.

differences in the $R_{Si–Si}$ value was obtained, which, when VdW interactions are taken into account, turns out to be 11.8% higher. The two optimization methods used give the greatest differences in the binding energies $\Delta E^{b}_{Si(P)}$ (11.4%) and $\Delta E^{b}_{C(N)}$ (6.3%) for systems (N_{Si} = 2, N_N = 2, N_P = 2) and (N_{Si} = 2, N_N = 0, N_P = 2), respectively, and the minimum differences in the same characteristics (4.8% and 5.0%) obtained in the case of the same system (N_{Si} = 1, N_N = 2, N_P = 2). The binding energies $E^{b}_{Si(P)}$ and $E^{b}_{C(N)}$ calculated using the PBE approximation are always higher than the corresponding characteristics determined using the (VdW-DF) DRSLL approximation. Thus, taking into account the *VdW* contribution to the interaction of silicene with a graphite substrate is most noticeable when calculating the adhesion energy between them, including after the NTD procedure was carried out for this system.

Silicene doped with phosphorus straightens, i.e., loses corrugation. The walls of the modified channel do not have buckles, even before filling the channel with lithium. To translate the obtained stresses into units of N m^{-1}, we assume that the thickness of one layer of modified silicene is 0.3 nm. Calculations show (Fig. 8) that the maximum tensile stress acting in the plane of sheets of modified silicene does not exceed 0.45 N/m. The maximum allowable tensile stress of silicene [18] exceeds the maximum local stress σ_{zy} calculated by us by 13 times. Therefore, lithium filling the channel does not have a destructive effect on its walls.

The maximum attainable stress σ_{zz} in the doped walls of the channel filled with lithium is 5 times less than the ultimate tensile stress for silicene. Thus, in spite of the high degree of expansion of the silicene channel doped with phosphorus during intercalation with lithium, it has a sufficient stability margin so as not to collapse.

The deformation associated with the displacement of P atoms from the sites created by vacancy defects, causes the strengthening of Si–C bonds due to the formation of a pz-like atomic orbital in silicon atoms. As a result, the reactivity of silicene is increased. A similar effect was observed upon compression deformation or high tension of silicene and was manifested in the strengthening of the sp^3 nature of Si–Si bonds [43].

Let us now analyze the effectiveness of the NTD procedure applied to the "two-layer silicene on a graphite substrate" system with respect to the intercalation of lithium into the channel formed by sheets of modified silicene. Despite a more than twofold change in the volume of this channel, its destruction during intercalation of lithium was not observed. The highest channel occupancy with lithium was achieved at a gap of h_g = 0.24 nm normal for two-dimensional silicene when its doping with phosphorus reached 6%. The found capacity with respect to lithium for such a channel is 2.6 times greater than the capacity for a similar channel of undoped silicene with the same number of bivacancies not filled with any atoms when the channel was on a nickel substrate [14]. For a silicene channel, of identical size and located on other metal substrates (Ag, Al, Cu), an even lower occupancy rate of lithium was obtained during intercalation than was the case for the channel on a nickel substrate [11–13]. Strong Si-P bonds increase the strength of the modified channel. The channel capacity in relation to filling with lithium increases until the phosphorus concentration in silicene exceeds 6%. Otherwise, the P atoms entering the channel, but connected with its walls, interfere with the intercalation of lithium, and the occupancy of the channel by Li atoms decreases sharply.

Conclusion

In this work, we studied the electronic and mechanical properties of a two-layer silicene on a graphite substrate after neutron transmutation doping of this system. We investigated the strength of the channel formed by modified silicene sheets with respect to its intercalation with lithium. It was found that silicene, which in an autonomous state is a narrow-gap semiconductor, when placed on a graphite substrate acquires conductive properties. This trend continues after the NTD procedure is performed on the "silicene on a graphite substrate" system. There is a possibility of the restoration of the semiconductor properties of two-dimensional silicon. To do this, it must be doped in a certain way and then placed on an undoped graphite substrate. The "double-layer silicene on graphite" system doped with the NTD method seems to be an effective material for use in the design of the anode of a lithium-ion battery. When a silicene channel is doped with phosphorus, and the concentration of P atoms does not exceed 6%, it can contain a significantly larger number of Li atoms during intercalation than is the case with a channel with undoped silicene walls located on different metal substrates. Moreover, the channel volume can increase by more than two times, which, however, does not lead to its destruction. An artificial increase in the volume of the modified silicene channel by increasing its gap up to 0.75 nm does not increase the capacity during intercalation of lithium. The appearance of conductivity in phosphorus-doped silicene on a graphite substrate favors the use of such an electrode in LIB, because helps increase battery charging speed. The mechanical stresses appearing in the walls of the modified silicene channel when it is filled with lithium do not exceed the corresponding stresses that arise during intercalation of lithium in a similar unalloyed silicene channel.

Thus, the electronic and mechanical properties of silicene necessary for its use as a LIB material can be significantly improved by pretreatment of this material by applying an NTD-controlled procedure.

Supplementary information

The stresses appearing in the phosphorus-doped silicene channel after it was filled with lithium were calculated by the classical molecular dynamics method. This computer experiment is described in more detail in Supplementary Materials. The calculations were carried out using the LAMMPS software package. The channel was located on a graphite substrate with 5% doping with nitrogen. Considered are 3%, 6%, 9%, and 18% doping of silicene sheets with phosphorus. Similar calculations were performed for the case of an unalloyed system. Each silicene sheet initially contained 300 Si atoms and had a size of 5.4 × 4.3 nm. To simulate the doped silicene structure, 9 vacancy defects of the type were formed in the sheets: mono-, bi-, tri-, and hexavacancies, which were then filled with phosphorus atoms. The distance between the sheets of bilayer silicene, calculated by the DFT method, was 0.24 nm. We studied the sequential (through the frontal plane $y0z$, $x = 0$—entrance to the channel) filling of channels with gaps from 0.24 nm to 0.75 nm by lithium ions launched individually into the channel every 1 ps. Ions moved under the influence of a constant electric field with a strength of 10^4 V m^{-1}. The field strength vector is directed along the $0x$ axis.

Acknowledgements

This work was carried out in the framework of agreement No. 075-03-2020-582/1 of 02/18/2020 (topic number 0836-2020-0037).

Author contributions

A.Y. Galashev performed conceptualization and methodology, formal analysis, investigation, writing—original draft preparation, project administration, funding acquisition. A.S. Vorob'ev engaged in investigation, software, validation, resources, data curation, formal analysis.

Compliance with ethical standards

Conflict of interest The authors declare that they have no conflict of interest.

Electronic supplementary material: The online version of this article (https://doi.org/10.1007/s10853-020-04860-8) contains supplementary material, which is available to authorized users.

References

[1] Jain V, Kandasubramanian B (2020) Functionalized graphene materials for hydrogen storage. J Mater Sci 55:1865–1903. https://doi.org/10.1007/s10853-019-04150-y

[2] Wang X, Shi Z, Meng F, Zhao Y, Wu Z, Lei Y, Xue L (2020) Interfacial interaction-induced temperature-dependent mechanical property of graphene-PDMS nanocomposite. J Mater Sci 55:1553–1561. https://doi.org/10.1007/s10853-019-04126-y

[3] Wu Y, Mu H, Cao X, He X (2020) Polymer-supported graphene–TiO2 doped with nonmetallic elements with enhanced photocatalytic reaction under visible light. J Mater Sci 55:1577–1591. https://doi.org/10.1007/s10853-019-04100-8

[4] Luo J, Gao T, Li L, Xie Q, Tian Z, Chen Q, Liang Y (2019) Formation of defects during fullerene bombardment and repair of vacancy defects in graphene. J Mater Sci 54:14431–14439. https://doi.org/10.1007/s10853-019-03938-2

[5] Kovalev AI, Wainstein DL, Tetelbaum DI, Hornig W, Kucherehko YN (2004) Investigation of the electronic structure of the phosphorus-doped Si and SiO2: Si quantum dots by XPS and HREELS methods. Surf Interface Anal 36:959–962

[6] Fujii M, Toshikiyo K, Takase Y, Yamaguchi Y, Hayashi S (2003) Below bulk-band-gap photoluminescence at room temperature from heavily P- and B-doped Si nanocrystals. J Appl Phys 94:1990–1995

[7] Kane BE (1998) A silicon-based nuclear spin quantum computer. Nature 393:133–137

[8] Debernardi A, Baldereschi A, Fanciulli M (2006) Computation of the Stark effect in P impurity states in silicon. Phys Rev B 74:035202

[9] Fujii M, Mimura A, Hayashi S (2002) Hyperfine structure of the electron spin resonance of phosphorus-doped Si nanocrystals. Phys Rev Lett 89:296805–296809

[10] Chen Q, Wang J, Zhang Y (2016) Activation energy study of phosphorus-doped microcrystalline silicon thin films. Optic 127:10437–10441

[11] Galashev AY, Ivanichkina KA (2018) Computer study of atomic mechanisms of intercalation/deintercalation of Li ions in a silicene anode on an Ag (111) substrate. J Electrochem Soc 165:A1788–A1796

[12] Galashev AY, Ivanichkina KA (2019) Computer test of a new silicene anode for lithium-ion battery. ChemElectroChem 6:1525–1535

[13] Galashev AY, Ivanichkina KA (2019) Computional investigation of a promising Si-Cu anode material. PCCP 21:12310–12320

[14] Galashev AY, Zaikov YuP (2019) New Si–Cu and Si–Ni anode materials for lithium-ion batteries. J Appl Electrochem 49:1027–1034

[15] Galashev AE, Ivanichkina KA (2019) Numerical simulation of the structure and mechanical properties of silicene layers on graphite during the lithium ion motion. Phys Solid State 61:233–243

[16] Galashev AE, Ivanichkina KA (2019) Computer modeling of lithium intercalation and deintercalation in a silicene channel. Russ J Phys Chem A 93:765–769

[17] Galashev AE, Vorob'ev AS (2018) Physical properties of silicene electrodes for Li-, Na-, Mg-, and K-ion batteries. J Solid State Electrochem 22:3383–3391

[18] Roman R, Cranford SW (2014) Mechanical properties of silicene. Comput Mater Sci 82:50–55

[19] Chung J-Y, Sorkin V, Pei Q-X, Chiu C-H, Zhang Y-W (2017) Mechanical properties and failure behaviour of graphene/silicene/graphene heterostructures. J Phys D Appl Phys 50:345302

[20] Galashev AE, Rakhmanova OR, Ivanichkina KA (2018) Graphene and graphite supports for silicone stabilization: a computer study. J Struct Chem 59:877–883

[21] Galashev AE, Ivanichkina KA (2017) Nanoscale simulation of the lithium ion interaction with defective silicene. Phys Lett A 381:3079–3083

[22] Galashev AE, Ivanichkina KA, Vorob'ev AS, Rakhmanova OR (2017) Structure and stability of defective silicene on Ag(001) and Ag(111) substrates: a computer experiment. Phys Solid State 59:1242–1252

[23] Rakhmanova OR, Galashev AE (2017) Motion of a lithium ion over a graphene–silicene channel: a computer model. Russ J Phys Chem A 91:921–925

[24] Tsoutsou D, Xenogiannopoulou E, Golias E, Tsipas P, Dimoulas A (2013) Evidence for hybrid surface metallic band in (4 × 4) silicene on Ag(111). Appl Phys Lett 103:231604

[25] Meng L, Wang Y, Zhang L, Du S, Wu R, Li L, Zhang Y, Li G et al (2013) Buckled silicene formation on Ir(111). Nano Lett 13:685–690

[26] Stpniak-Dybala A, Dyniec P, Kopciuszyski M, Zdyb R, Jałochowski M, Krawiec M (2019) Planar silicene: A new silicon allotrope epitaxially grown by segregation. Adv Funct Mater 29:1906053

[27] Cai Y, Chuu CP, Wei CM, Chou MY (2013) Stability and electronic properties of two-dimensional silicene and germanene on graphene. Phys Rev B 88:245408

[28] Houssa M, Dimoulas A, Molle A (2015) Silicene: a review of recent experimental and theoretical investigations. J Phys Condens Matter 25:253002

[29] De Crescenzi M, Berbezier I, Scarselli M, Castrucci P, Abbarchi M, Ronda A, Jardali F, Park J, Vach H (2016) Formation of silicene nanosheets on graphite. ACS Nano 10:11163–11171

[30] An Y, Hou Y, Gong S, Wu R, Zhao C, Wang T, Jiao Z, Wang H, Liu W (2020) Evaluating the exfoliation of two-dimensional materials with a Green's function surface model. Phys Rev B 101:075416

[31] Podsiadly-Paszkowska A, Krawiec AM (2015) Silicene on metallic quantum wells: An efficient way of tuning silicene-substrate interaction. Phys Rev B 92:165411

[32] Zeng Z, Ma X, Chen J, Zeng Y, Yang D, Liu Y (2010) Effects of heavy phosphorous-doping on mechanical properties of Czochralski silicon. J Appl Phys 107:123503

[33] Okamoto S, Ito A (2012) Investigation of mechanical properties of nitrogen-containing graphene using molecular dynamics simulations, Proceeding of the international multy conference of engineers and computer scientists, vol 1. IMECS, Hong Kong

[34] Solera JM, Artacho E, Gale JD, García A, Junquera J, Ordejon P, Sanchez-Portal D (2002) The SIESTA method for ab initio order-N materials simulation. J Phys Condens Matter 14(11):2745–2779

[35] Hu W, Li Z, Yang J (2013) Structural, electronic, and optical properties of hybrid silicene and graphene nanocomposite. J Chem Phys 139:154704

[36] Joo Y, Kim M, Kanimozhi C, Huang P, Wong BM, Roy SS, Arnold MS, Gopalan P (2016) Effect of dipolar molecule structure on the mechanism of graphene-enhanced Raman scattering. J Phys Chem C 120(25):13815–13824

[37] Huang C, Kim M, Wong BM, Safron NS, Arnold MS, Gopalan P (2014) Raman enhancement of a dipolar molecule on graphene. J Phys Chem C 118(4):2077–2084

[38] Dion M, Rydberg H, Schroder E, Langreth DC, Lundqvist BI (2004) Van der Waals density functional for general geometries. Phys Rev Lett 92:246401

[39] Galashev AY (2015) Computer study of the removal of Cu from the graphene surface using Ar clusters. Comp Mater Sci 98:123–128

[40] Bin Hamid MA, Tim CK, Bin Yaakob Y, Bin Hazan MA (2019) Structural, electronic and transport properties of silicene on graphene substrate. Mater Res Exp 6(5):055803

[41] Zhou R, Lew Yan Voon LC, Zhuang Y (2013) Properties of two-dimensional silicon grown on graphene substrate. J Appl Phys 114:093711

[42] Perdew JP, Burke K, Ernzerhof M (1996) Generalized gradient approximation made simple. Phys Rev Lett 77:3865–3868

[43] Marjaoui A, Stephan R, Hanf M-C, Diani M, Sonnet P (2017) Using strain to control molecule chemisorption on silicene. J Chem Phys 147:044705